KLHL3 regulates paracellular chloride transport in the kidney by ubiquitination of claudin-8

Yongfeng Gong[a,b], Jinzhi Wang[a,b], Jing Yang[a,b], Ernie Gonzales[c], Ronaldo Perez[c], and Jianghui Hou[a,b,1]

Departments of [a]Internal Medicine–Renal Division and [c]Neurology and [b]Center for Investigation of Membrane Excitability Diseases, Washington University Medical School, St. Louis, MO 63110

Edited by Martin R. Pollak, Harvard University, Brookline, MA, and approved March 2, 2015 (received for review November 29, 2014)

A rare Mendelian syndrome—pseudohypoaldosteronism type II (PHA-II)—features hypertension, hyperkalemia, and metabolic acidosis. Genetic linkage studies and exome sequencing have identified four genes—with no lysine kinase 1 (wnk1), wnk4, Kelch-like 3 (KLHL3), and Cullin 3 (Cul3)—mutations of which all caused PHA-II phenotypes. The previous hypothesis was that the KLHL3–Cul3 ubiquitin complex acted on the wnk4–wnk1 kinase complex to regulate Na^+/Cl^- cotransporter (NCC) mediated salt reabsorption in the distal tubules of the kidney. Here, we report the identification of claudin-8 as a previously unidentified physiologic target for KLHL3 and provide an alternative explanation for the collecting duct's role in PHA-II. Using a tissue-specific KO approach, we have found that deletion of claudin-8 in the collecting duct of mouse kidney caused hypotension, hypokalemia, and metabolic alkalosis, an exact mirror image of PHA-II. Mechanistically, the phenotypes in claudin-8 KO animals were caused by disruption of the claudin-8 interaction with claudin-4, the paracellular chloride channel, and delocalization of claudin-4 from the tight junction. In mouse collecting duct cells, knockdown of KLHL3 profoundly increased the paracellular chloride permeability. Mechanistically, KLHL3 was directly bound to claudin-8, and this binding led to the ubiquitination and degradation of claudin-8. The dominant PHA-II mutation in KLHL3 impaired claudin-8 binding, ubiquitination, and degradation. These findings have attested to the concept that the paracellular pathway is physiologically regulated through the ubiquitination pathway, and its deregulation may lead to diseases of electrolyte and blood pressure imbalances.

chloride | ion channel | nephrology | tight junction | ubiquitination

Gordon's syndrome, also known as pseudohypoaldosteronism II (PHA-II) or familial hyperkalemic hypertension, features several metabolic derangements, including hypertension, hyperkalemia, and hyperchloremic metabolic acidosis (1). Mutations in four genes have been found to cause Gordon's syndrome. Two encode the serine-threonine kinases with no lysine kinases (WNKs) (2). The other two encode proteins important in the cullin-really interesting new gene E3 ubiquitin ligase (CRL) complex—Kelch-like 3 (KLHL3) and Cullin 3 (CUL3) (3, 4). Disease-causing mutations in WNKs are dominant and confer gain of function to augment NaCl reabsorption in the distal convoluted tubule (DCT) by a signaling cascade of SPAK/OSR1 to NCC (5, 6). Mutations in KLHL3 are either recessive or dominant. Recessive mutations include premature termination, frameshift, and splicing alternatives, consistent with loss of function, whereas dominant mutations cluster in the β-propeller domain important in target recognition (3, 4). CUL3 mutations are all dominant and de novo and result in the skipping of exon 9 and in-frame deletion of a 57-aa segment important in maintaining the CRL architecture (3). KLHL3 was found to interact with WNK4 and regulate its ubiquitination and degradation (7, 8). Presumably, loss of KLHL3 function may lead to increases in WNK4 protein levels that, in turn, promote NCC phosphorylation and NaCl reabsorption in the DCT. Compatible with this notion, a knock-in mouse model harboring a dominant mutation (R528H) allele in the KLHL3 gene developed PHA-II–related phenotypes and concomitant increases in WNK4 protein abundance and NCC phosphorylation levels (9).

All four PHA-II genes have significant expression in renal tubules, including the DCT, the connecting tubule (CNT), and the collecting duct (CD) (2, 3). Although the PHA-II mechanism in the DCT has been extensively studied, the CNT/CD's role remains largely elusive. The predominant NaCl transport pathway in the CNT/CD is through epithelial Na^+ channel (ENaC) mediated Na^+ reabsorption and electrically coupled paracellular Cl^- reabsorption (also known as the chloride shunt) (10, 11). WT WNK4 inhibits ENaC conductivity, whereas PHA-II–causing mutations eliminate WNK4's inhibition of ENaC, thereby promoting Na^+ reabsorption in the CNT/CD (12). The disease-causing mutation in WNK4 has also been found to augment paracellular Cl^- conductance in renal epithelial cells (13, 14). The hypothesis of unopposed chloride shunt is particularly important to explain hyperchloremia and hyperkalemia in PHA-II. The shunt conductance would favor Cl^- reabsorption and decrease the lumen-negative transepithelial voltage as the driving force for K^+ secretion (15). To reveal the molecular nature of chloride shunt and its potential role in PHA-II pathophysiology, we have generated the KO mouse models for two claudin molecules—claudin-4 and claudin-8—both of which are required to generate paracellular Cl^- conductance in vitro (16). The claudin-4 KO mice developed hypotension, hypochloremia, and metabolic alkalosis because of renal loss of Cl^- (11). The claudin-8 KO phenocopied claudin-4 KO, which can be mechanistically attributed to their interaction and coassembly into the tight junction (TJ). Most intriguingly, KLHL3 directly interacted with claudin-8 and regulated its ubiquitination and degradation. Loss of KLHL3 in the CD cells increased the TJ conductance to chloride. The dominant PHA-II mutation in KLHL3 abolished its interaction and regulation of claudin-8. These findings have revealed a previously unidentified physiological substrate for KLHL3 and provided important insights of the TJ's role in PHA-II pathogenesis.

Significance

The role of tight junction permeability in causing human diseases is an important but understudied area. Here, we discovered a previously unidentified mechanism in the kidney that uses the Kelch-like 3-dependent ubiquitination pathway to regulate claudin-8 and the paracellular permeability to chloride. The importance of posttranslational regulation of tight junction structure and function is shown here, with emphasis on its potential role in causing human hypertension if a proper ubiquitination pathway is disrupted by genetic mutations. Such a mechanism may also be explored as a pharmacologic tool to correct tight junction permeability defects and related diseases.

Author contributions: J.H. designed research; Y.G., J.W., J.Y., E.G., R.P., and J.H. performed research; Y.G. and J.H. analyzed data; and Y.G. and J.H. wrote the paper.

The authors declare no conflict of interest.

This article is a PNAS Direct Submission.

[1]To whom correspondence should be addressed. Email: jhou@wustl.edu.

This article contains supporting information online at www.pnas.org/lookup/suppl/doi:10.1073/pnas.1421441112/-/DCSupplemental.

Results

Generation of CD-Specific KO Animals of Claudin-8. Claudin-8 is expressed in the skin (17), the intestine (18), and the blood vessel (19) in addition to the kidney (16). To determine its kidney-specific role independent of any extrarenal effect, we have adopted the loxP/Cre strategy to generate conditional KO mouse models for claudin-8. *SI Appendix*, Fig. S1*A* shows the WT claudin-8 locus, the targeting construct, and the targeted locus. Exon 1 (only exon) of claudin-8 is flanked by two loxP sites. The phosphoglycerate kinase (PGK)-neo expression cassette is flanked by two flippase (flp) recognition target (FRT) sites. The correctly targeted ES cell clones (*SI Appendix*, Fig. S1 *B–D*) all showed normal karyotypes and were injected into the C57BL/6 blastocysts to generate chimera founders. The targeted allele was captured in the F1 generation derived from all chimera founders (*SI Appendix*, Fig. S1*E*), indicating successful germ-line transmission. Cleavage of PGK-neo was carried out by crossing F1 with a transgenic mouse line [129S4/SvJaeSor-Gt (ROSA)26Sor$^{tm1(FLP1)}$; Jackson Lab] that expresses the flp recombinase in the ROSA locus (*SI Appendix*, Fig. S1*E*). Capture of both floxed alleles was achieved by intercross of claudin-8$^{flox/+}$ heterozygous animals that had been backcrossed to the C57BL/6 background for five generations (*SI Appendix*, Fig. S1*E*). The claudin-8$^{flox/flox}$ animals were then crossed to the Aquaporin-2^{Cre} (Aqp2^{Cre}) hemizygous transgenic mice [established on C57BL/6 background; B6.Cg-Tg(Aqp2^{Cre})1Dek/J; Jackson Lab] that expressed the Cre recombinase under the Aqp2 promoter.

To definitively reveal the cellular localization pattern of claudin-8 along the nephron, we performed rigorous colocalization analyses for claudin-8 protein using molecular markers against each nephron segment—the proximal tubule, the thick ascending limb of the Henle's loop, the DCT, the CNT, and the CD. In claudin-8$^{flox/flox}$ (control) mouse kidneys, claudin-8 proteins were detected in tubules absent of the *Lotus tetragonolobus* lectin (a proximal convoluted/straight tubule marker) (*SI Appendix*, Fig. S2*A*) or the claudin-19 protein (a thick ascending limb of the Henle's loop marker) (*SI Appendix*, Fig. S2*B*) (20). Claudin-8 expression was present in the tubules labeled with the NCC protein (a DCT marker) (*SI Appendix*, Fig. S2*C*) (21) and extended to the CNT and the CD that were counterstained with Aqp2 (a CNT/CD marker) (Fig. 1*A*) (22). The renal tubular localization pattern of claudin-8 was consistent with the findings made by Li et al. (23) using different claudin-8 antibody and tubular markers (23). Because the CNT/CD is a heterogeneous epithelium made of the principal cell (PC) and the intercalated cell (IC), we used Aqp2 (a PC marker) to further discern claudin-8 expression pattern in PCs and ICs. Pendrin, an IC marker used in our previous studies (11), was not applicable here, because both pendrin and claudin-8 antibodies were raised in the same species. In control mouse kidneys, claudin-8 proteins were found in homotypic TJs between the PCs (Aqp2-positive cells) (Fig. 1*B*) as well as in heterotypic TJs between PCs and ICs (Aqp2-positive and -negative cells) (Fig. 1*B*), suggesting that both PCs and ICs expressed claudin-8. The claudin-8 expression in ICs had been reported before based on colocalization with an IC marker—H^+-ATPase (23). With the Aqp2 promoter-driven *Cre* allele, several CNT/CD-specific KO mouse models have been successfully generated [e.g., the ENaC KO (24), the mineralocorticoid receptor KO (25), and the claudin-4 KO (11)]. In claudin-8$^{flox/flox}$/Aqp2^{Cre} (KO) mouse kidneys, claudin-8 expression was selectively deleted in the Aqp2-positive CNT/CD tubules (Fig. 1*C*). Because Aqp2 was only expressed by the PC, the Aqp2-negative IC seemed to retain very low-level claudin-8 expression (Fig. 1*D*), suggesting that the heterotypic TJ requires the *trans*-interaction from the claudin molecules located in both contributing cells. Histologic analyses revealed no morphological abnormalities in the CNT/CD of KO animals (*SI Appendix*, Fig. S3). Together, these results have shown successful deletion of the claudin-8 gene specifically in the CD system.

Claudin-8 KO Mice Developed Renal Salt Wasting Defects and Low Blood Pressure. The age-matched (10- to 12-wk-old) CNT/CD-specific KO mice of claudin-8 (claudin-8$^{flox/flox}$/Aqp2^{Cre}) and control mice (claudin-8$^{flox/flox}$) were maintained on a regular salt diet (0.24% Na^+ and 0.30% Cl^-) and subjected to 24-h metabolic cage analyses. There was no significant difference in body weight between KO and control animals (Table 1). The KO animals developed hypochloremia—significantly reduced plasma Cl^- level (P_{Cl}) (Table 1)—but their plasma Na^+ level (P_{Na}) (Table 1) was not different from control. Because hypochloremia was often accompanied by alkalosis, we measured the arterial pH and HCO_3^- (P_{HCO3}) levels in both animal groups. Although the arterial pH was similar between KOs and controls, the P_{HCO3} was significantly higher in KO than control animals (Table 1). Notably, the plasma K^+ level (P_K) (Table 1) in KO animals was significantly reduced, indicating hypokalemia. The urinary excretion rates for Cl^- were significantly increased in KO animals: fractional excretion of Cl^- (FE_{Cl}) increased by 1.72-fold and absolute excretion of Cl^- (E_{Cl}) increased by 1.67-fold compared with controls (Table 1). The urinary excretion rates for Na^+ were also significantly higher in KO than control animals, with FE_{Na} increased by 1.49-fold and

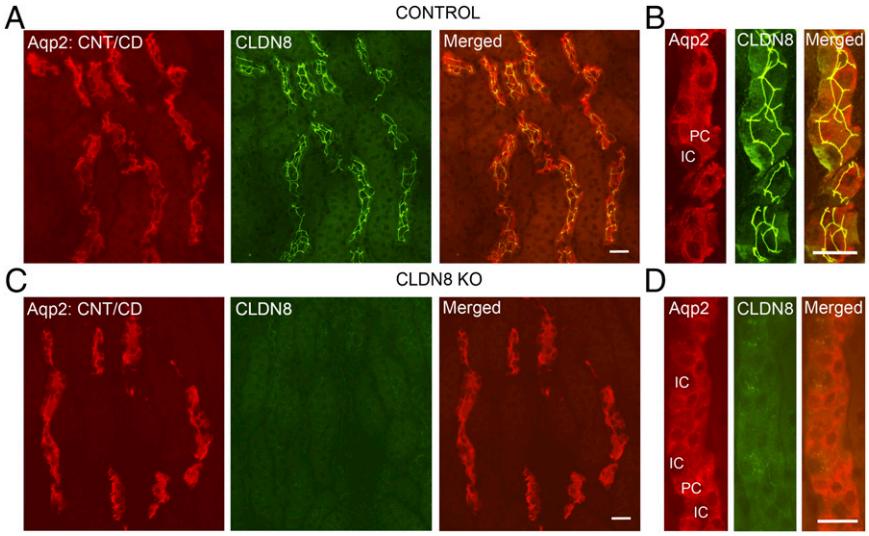

Fig. 1. CLDN8 cellular localization pattern in (*A* and *B*) control and (*C* and *D*) Aqp2-Cre–driven KO mouse kidneys. (*A*) Low and (*B*) high magnification views of double staining of CLDN8 with a CNT/CD marker, Aqp2, in the cortical medullar ray from the outer medulla to the cortex of the control mouse kidney. (*C* and *D*) Corresponding view of double staining of CLDN8 with Aqp2 in the KO mouse kidney. (Scale bar: 20 μm.)

Table 1. Plasma and urine electrolyte levels in claudin-8 KO and its control animals

Group	CLDN8$^{flox/flox}$	CLDN8$^{flox/flox}$/Aqp2^{Cre}	Significance (n = 15)
Weight, g	21.78 ± 0.53	20.52 ± 0.51	n.s.
Urinary volume, μL/24 h per gram	52.05 ± 5.75	69.56 ± 3.26	P = 0.008
U_{Osm}, Osm/kg	1.463 ± 0.085	1.435 ± 0.097	n.s.
C_{Cr}, mL/24 h per gram	3.51 ± 0.45	3.59 ± 0.24	n.s.
Mean BP, mmHg	109.9 ± 4.5	92.3 ± 1.7	P = 0.0007
pH	7.47 ± 0.01	7.46 ± 0.02	n.s.
P_{HCO3}, mmol/L	22.4 ± 0.7	25.3 ± 0.7	P = 0.014
P_{Aldo}, pg/mL	370.3 ± 37.8	549.4 ± 29.9	P = 0.005
P_{Cl}, mmol/L	106.0 ± 0.91	102.7 ± 0.82	P = 0.017
P_{Na}, mmol/L	141.6 ± 1.4	140.6 ± 1.0	n.s.
P_K, mmol/L	4.21 ± 0.10	3.90 ± 0.07	P = 0.016
FE_{Cl}, %	1.12 ± 0.16	1.93 ± 0.21	P = 0.013
E_{Cl}, μmol/24 h per gram	3.93 ± 0.71	6.55 ± 0.65	P = 0.016
FE_{Na}, %	0.89 ± 0.09	1.33 ± 0.13	P = 0.020
E_{Na}, μmol/24 h per gram	4.05 ± 0.42	6.10 ± 0.52	P = 0.008
FE_K, %	12.60 ± 1.72	22.07 ± 3.04	P = 0.021
E_K, μmol/24 h per gram	1.76 ± 0.27	2.94 ± 0.29	P = 0.014

n.s., not significant.

E_{Na} increased by 1.51-fold (Table 1). The renal handling of K^+ was particularly interesting. In contrast to the claudin-4 KO mice that were without any K^+ deregulation (11), the claudin-8 KO mice showed significant renal wasting of K^+, and their FE_K and E_K values were 1.75- and 1.67-fold, respectively, higher than in controls (Table 1). Despite significant urinary volume loss (Table 1), the urinary osmotic pressure (U_{Osm}) (Table 1) was unchanged in KO, indicating that these animals retained intact water handling capability. The creatinine clearance (C_{Cr}) rates (Table 1) were well-defended in KO animals, suggesting normal tubuloglomerular feedback responses in the face of renal salt and volume losses. Because renal salt and volume losses would induce changes in blood pressure (BP), we carefully monitored the BP levels in both anesthetized and awake animals. To record BP in anesthetized animals, intraarterial measurements were performed with catheters inserted into the carotid artery. The mean BP in KO was 17.6 mmHg lower than in control animals (P = 0.0007) (Table 1). To record BP in awake and unrestrained animals, sex- (male) and age-matched (12-wk-old) KO and littermate control mice were implanted with radiotelemetric transducers in the carotid artery (11). The 24-h telemetric traces showed that the mean BP in KO was consistently lower than in control animals throughout the 24-h period, with statistical significance reached for each time point (*SI Appendix*, Fig. S4). Hypotension caused by volume depletion would activate the renin–angiotensin–aldosterone axis, resulting in increased aldosterone synthesis. Compatible with this concept, the plasma aldosterone level (P_{Aldo}) was significantly increased by 1.48-fold in KO compared with control animals (Table 1). Together, these results have revealed a renal phenotype in claudin-8 KO animals related to salt, volume, and BP regulation.

Claudin-8 Was Required for Claudin-4 Localization to the TJ in the Kidney. The phenotypic similarities between claudin-8 KO and claudin-4 KO animals suggest that they may be within the same molecular pathway. Our previous genetic screening using yeast two-hybrid system and biochemical experiments carried out in mouse CD epithelia revealed direct protein interactions between claudin-8 and caudin-4 (16). Knowing from our previous studies of claudin-16 KO and claudin-19 KO animals that claudin interactions were required for their trafficking and coassembly into the TJ (26), we asked whether the TJ localization of claudin-4 required claudin-8 in the mouse kidneys and vice versa. In the CNT/CD of the claudin-8 KO mouse kidneys, claudin-4 staining almost completely disappeared, giving way to faint remnants of TJ strands that were discontinuous and had signal intensity not different from the background level (arrows in Fig. 2*A*), contrasting the TJ patterns in the control kidneys (Fig. 2*A*). However, the TJ localization of claudin-8 protein was not affected in the CDs of claudin-4 KO mouse kidneys (Fig. 2*B*), suggesting claudin-8 had additional interaction partners. Indeed, from our previous quantitative interaction measurements, claudin-8 showed similarly strong affinities for not only claudin-4 but also claudin-3 and claudin-7; loss of claudin-4 did not inhibit claudin-8 binding to these other claudins (16). Claudin-4 only interacted with claudin-8; therefore, loss of claudin-8 exerted a predominant effect on claudin-4's localization (16). Because the deletion of claudin-8, in fact, created a double KO at the level of TJ, we then asked whether the barrier function or the TJ integrity was affected in the CNT/CD of claudin-8 KO animals. From the previous in vitro recording (16) and the in vivo KO study (27), claudin-7 functioned as a nonselective barrier to ion movement across the CNT/CD TJ. We stained claudin-7 proteins in claudin-8 KO mouse kidneys and found no difference from its localization pattern in control animals (*SI Appendix*, Fig. S5*A*), suggesting that the barrier function of the CD remained intact in the absence of claudin-8. The ZO-1 protein, being the most widely accepted marker for TJ integrity, was stained in both claudin-8 KO and control mouse kidneys. The ZO-1 localization revealed grossly normal TJ patterns in terms of strand continuity, shape, and signal intensity in the CNT/CD of claudin-8 KO compared with control animals (*SI Appendix*, Fig. S5*B*), suggesting intact TJ integrity. Together, these results have shown the in vivo requirement of claudin interaction in TJ assembly and architecture.

KLHL3 Regulated Chloride Shunt Permeability by Claudin-8. Several previous studies have identified a regulatory role for WNKs in chloride shunt permeabilities (13, 14). Knowing that KLHL3 had substantial expression in the CD (28), we asked whether KLHL3, the most frequently mutated gene in PHA-II, would directly regulate chloride shunt conductance. siRNA molecules against KLHL3 were transfected into the mouse CD cells M-1 and mIMCD3 using a retroviral delivery system (29). The siRNA molecules were designed by the siDESIGN Center at Thermo Scientific as described previously (11). Four independent siRNA sequences (293, 805, 928, and 1,674) (*SI Appendix, Materials and Methods*) were tested in M-1 and mIMCD3 cells. All showed over 50% knockdown (KD) of KLHL3 mRNA levels, with

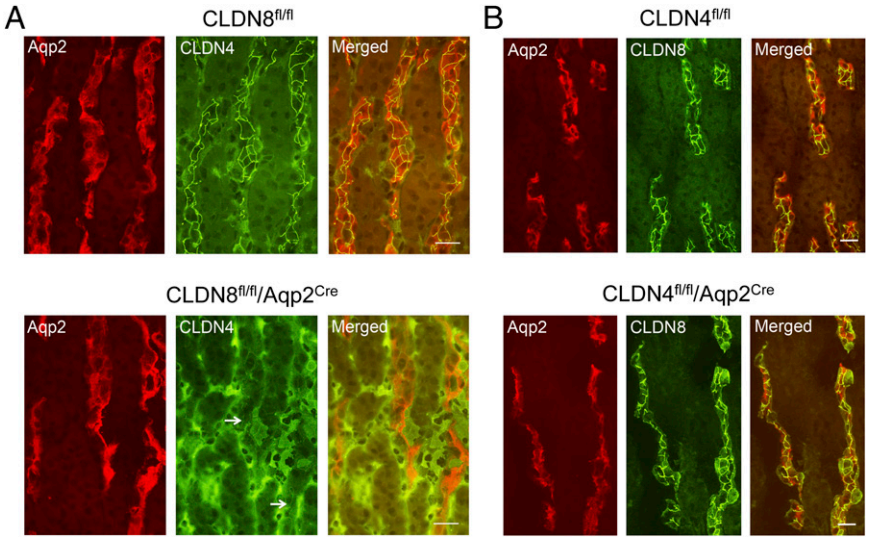

Fig. 2. CLDN4 and CLDN8 cellular localization in CLDN8 KO and CLDN4 KO mouse kidneys, respectively. (*A*) Comparison of CLDN4 localization pattern in Aqp2-positive tubules between CLDN8 KO and CLDN8$^{fl/fl}$ animals. Arrows denote remnant CLDN4 TJ strands in CLDN8 KO kidneys (where longer exposure time was taken for the CLDN4 signal to be seen). (*B*) Comparison of CLDN8 localization pattern in Aqp2-positive tubules between CLDN4 KO and CLDN4$^{fl/fl}$ animals. (Scale bar: 20 μm.)

siRNA-1,674 achieving ~90% KD efficacy (*SI Appendix*, Fig. S6). To record paracellular permeabilities independent of membrane conductance, we used a mixture of membrane ion channel/transporter blockers described before (*SI Appendix, Materials and Methods*) (amiloride for ENaC, bumetanide for NKCC1, DIDS for anion channels, and niflumic acid for pendrin) (16). In both M-1 and mIMCD3 cells, KD of KLHL3 with siRNA-1,674 significantly reduced the transepithelial resistance (TER) by 43% and 18%, respectively, compared with scrambled siRNA (control) (*SI Appendix*, Table S1). The voltage–current curve was linear in both KD and control cells, indicating predominant paracellular effects. To reveal the changes in paracellular ion selectivity, dilution potential (DP) measurements were performed on KD and control cell monolayers (with the luminal membrane as zero reference), allowing the calculation of anion selectivity (P_{Cl}/P_{Na}) with the Goldman–Hodgkin–Katz equation (*SI Appendix, Materials and Methods*). Across both M-1 and mIMCD3 cell monolayers, KD of KLHL3 reversed the sign of DP (*SI Appendix*, Table S1), transforming a slightly cation-selective paracellular pathway into a highly anion-selective pathway (*SI Appendix*, Table S1). The changes in ion selectivity were caused by profound increases in paracellular chloride permeability (P_{Cl} by 2.4- and 1.5-fold in M-1 and mIMCD3, respectively) (Fig. 3*A* and *SI Appendix*, Table S1), whereas paracellular sodium permeability (P_{Na}) was not affected. Because the M-1 cells showed more pronounced changes in P_{Cl} after KLHL3 KD, we chose this cell model to further investigate how overexpression of KLHL3 or its dominant mutation R528H found in PHA-II would affect chloride shunt conductance. Consistent with the KD data that KLHL3 functioned as a negative regulator of chloride shunt permeability, overexpression of WT KLHL3 significantly increased the TER and the DP (*SI Appendix*, Table S2) but reduced the P_{Cl} (Fig. 3*B* and *SI Appendix*, Table S2). The R528H mutant, however, exerted the opposite effect to WT KLHL3 by decreasing the TER, reversing the ion selectivity (*SI Appendix*, Table S2), and increasing the P_{Cl} (Fig. 3*B* and *SI Appendix*, Table S2). Notably, the paracellular permeability changes in cells expressing the R528H mutant were similar to those in KD cells, although with a smaller effect size, suggesting that the R528H mutation played dominant negative roles. To determine whether claudin-8 was required for KLHL3 function as additional evidence to support the direct interaction hypothesis between these two molecules (vide infra), we generated the claudin-8 siRNA KD M-1 cells as described before (16). In claudin-8 KD cells, overexpression of neither WT nor mutant KLHL3 was able to significantly alter P_{Cl} (Fig. 3*B* and *SI Appendix*, Table S2). Together, these results have provided functional support to the concept that KLHL3 directly regulated chloride shunt conductance through regulation of claudin-8.

KLHL3 Binding, Ubiquitination, and Degradation of Claudin-8. Because the intracellular C-terminal domain of claudin-8 protein is enriched with lysine (K) residues (*SI Appendix*, Fig. S7), we asked whether ubiquitination might represent a novel means of claudin regulation. KLHL3 in the CRL complex mediates target recognition through binding to its Kelch domain. We first tested whether claudin-8 was a binding partner of KLHL3 in HEK293 cells that normally lacked the expression of both claudin and KLHL3. In doubly transfected cells, anti-KLHL3 was able to precipitate claudin-8, whereas anti-claudin-8 antibody reciprocally precipitated

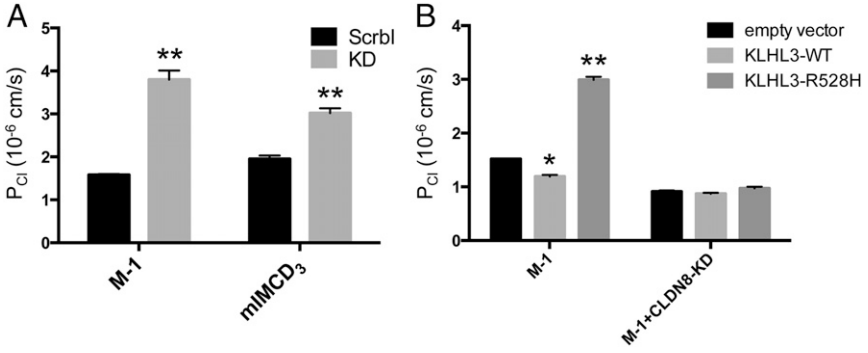

Fig. 3. Effects of KLHL3 manipulation on paracellular ion permeation. (*A*) KLHL3 KD mediated by siRNA-1,674 altered the Cl^- permeability (P_{Cl}) across the M-1 and mIMCD3 cell monolayers. $n = 3$. $^{**}P < 0.01$ relative to scrambled (Scrbl) siRNA. (*B*) Overexpression of WT KLHL3 or it R528H mutant altered P_{Cl} in M-1 cells. Claudin-8 KD abolished the KLHL3 overexpression effects. $n = 3$. $^{*}P < 0.05$; $^{**}P < 0.01$ relative to empty vector expression.

CELL BIOLOGY

KLHL3 (Fig. 4*A*). The R528H mutation in KLHL3, a frequent dominant mutation found in PHA-II, affects the proper folding of its Kelch domain and in theory, the binding to its target proteins. Compatible with this concept, the R528H mutation diminished the binding affinity between KLHL3 and claudin-8 by ∼40% (Fig. 4*B*). The binding of KLHL3 to claudin strongly suggested that KLHL3 may promote claudin ubiquitination and degradation. Accordingly, we determined claudin protein expression levels in the absence or presence of KLHL3 in cultured mouse CD cells—the M-1 cells. As shown in Fig. 4*C*, KD of KLHL3 as described elsewhere in this study significantly increased the protein level of claudin-8 in M-1 cells. In contrast, KLHL3 overexpression clearly reduced the protein abundance of claudin-8 in M-1 cells (Fig. 4*D*). We next tested whether the R528H mutation could abolish the KLHL3 regulation of claudin-8 protein abundance. In M-1 cells, transfection of the R528H mutant resulted in a higher expression level of claudin-8 compared with either WT KLHL3 or empty vector transfected cells (Fig. 4*D*), indicating a dominant negative effect. The level of claudin-8 ubiquitination was determined with a monoclonal ubiquitin antibody. As shown in Fig. 4*E*, claudin-8 proteins from M-1 cells were ubiquitinated, presumably through endogenous KLHL3. Transfection of WT KLHL3 significantly increased the ubiquitinated claudin-8 fraction (Fig. 4*E*). The R528H mutant reduced the fraction of ubiquitinated claudin-8 protein (Fig. 4*E*) compared with either WT KLHL3 or empty vector-transfected cells. Considering that the total abundance of claudin-8 protein was much higher in R528H-transfected cells (Fig. 4*D*), the ratio of ubiquitinated vs. total claudin-8 abundance was, in fact, much lower in R528H than in WT KLHL3 or empty vector-transfected cells, further confirming the dominant negative effect. Finally, we asked which amino acid locus in claudin-8 protein was ubiquitinated. There are four lysine residues in the intracellular C-terminal domain of human claudin-8: K191, K207, K213, and K214 (*SI Appendix*, Fig. S7). We have systematically mutated them into arginine and tested the expression levels of these mutant proteins in the absence or presence of KLHL3 in M-1 cells. As shown in Fig. 4*F*, the K213R mutant was resistant to KLHL3-induced down-regulation of claudin-8, suggesting that the K213 locus was where ubiquitination took place. Moreover, K213 is the only conserved lysine residue across different mammalian claudin-8 protein sequences (*SI Appendix*, Fig. S7), suggesting that the ubiquitination-based claudin regulation is evolutionarily conserved. Together, these results have established the underlying mechanism of KLHL3-mediated claudin regulation.

Discussion

The mechanism of PHA-II has been under debate for many years. The high sensitivity of both hypertension and metabolic abnormalities to thiazide has been interpreted as reflecting salt hyperreabsorption through the thiazide-sensitive transporter—NCC in the DCT (1). The PHA-II–causing mutations in WNKs increased membrane abundance levels of NCC in vitro in *Xenopus* oocytes (6). Transgenic mice harboring a knock-in mutant allele (D561A) of WNK4 as an in vivo model for PHA-II showed increases in NCC protein levels in the apical membrane of DCT cells (30). Susa et al. (9) reported the generation of a new PHA-II animal model by knocking in a mutant allele (R528H) of KLHL3 and found a similar increase in NCC membrane abundance levels in the DCT. Nevertheless, transgenic overexpression of NCC in the DCT alone was not able to induce any PHA-II phenotype, likely because of the lack of phosphorylated NCC (31). More intriguingly, the kidney-specific deletion of Cul3 in mice caused chronic hypotension, despite increases in WNK4 protein abundance and NCC phosphorylation (28). Although the mechanisms related to how WNK4 mutations cause PHA-II are well-established, the pathogenic mechanisms for KLHL3 mutations are far from clear. WNK4 protein, as a genuine substrate of KLHL3, is predicted to have higher abundance levels in patients harboring KLHL3 mutations. However, transgenic overexpression of WNK4 caused low BP and hypochloremia, opposite to the PHA-II phenotypes (32). Apparently, PHA-II is a multifaceted disease altering the functions of many more transport proteins. Schambelan et al. (15) have proposed an alternative hypothesis for PHA-II based on abnormalities in the CD that may result from an unopposed chloride shunt. The chloride shunt conductance would accompany sodium reabsorption

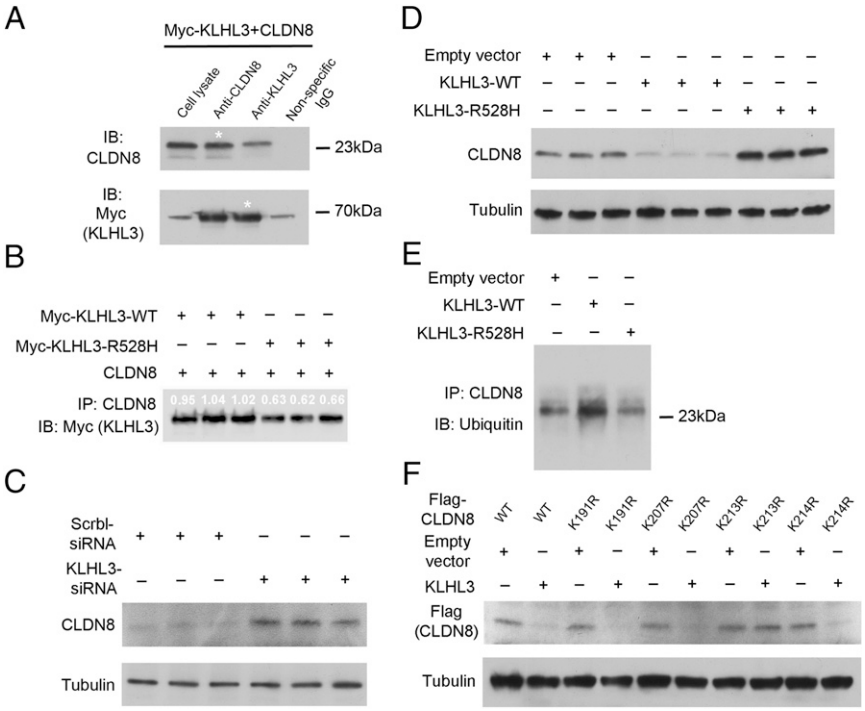

Fig. 4. KLHL3 regulation of CLDN8 in kidney epithelial cells. (*A*) Coimmunoprecipitation of WT KLHL3 with CLDN8 in HEK293 cells. Antibodies used for immunoprecipitation are shown above the lanes; antibody for blot visualization is shown on the left. *Lane shows 10% of input amount as in other lanes. (*B*) Comparison of interaction strength between WT KLHL3 with CLDN8 and R528H KLHL3 with CLDN8. (*C*) Cellular abundance level of CLDN8 in M-1 cells transfected with KLHL3 siRNA. (*D*) Cellular abundance level of CLDN8 in M-1 cells transfected with WT KLHL3, R528H KLHL3, or empty vector. (*E*) CLDN8 ubiquitination levels in M-1 cells transfected with WT KLHL3 or R528H KLHL3. Ubiquitinated CLDN8 was first immunoprecipitated with anti-CLDN8 antibody and then detected with anti-ubiquitin antibody. (*F*) Cellular abundance level of CLDN8 in M-1 cells cotransfected with KLHL3 and WT or lysine mutation CLDN8. IB, immunoblot; IP, immunoprecipitation; nonspecific antibody, anti-CLDN1; Scrbl, scrambled.

through ENaC and decrease the lumen-negative potential that drives potassium secretion. Notably, the two PHA-II animal models based on the knock-in mutation of WNK4 or KLHL3 both showed up-regulation of ENaC expression in the CD (9, 32). The same WNK4 mutant also augmented chloride shunt conductance (13, 14). We now provide compelling evidence that KLHL3 regulates chloride shunt conductance through direct binding and ubiquitination of claudin-8, which interacts with and recruits claudin-4 to the TJ.

The claudin-8 KO and claudin-4 KO animals share similar phenotypes, emphasizing the importance of claudin interaction in causing diseases. A similar example can be found in the case of familial hypomagnesemia with hypercalciuria and nephrocalcinosis (FHHNC) syndrome caused by the disruption of claudin-16 and claudin-19 interaction (26, 33). Notably, the hypotensive phenotype of claudin-8 KO animals seemed more severe than that of claudin-4 KO. Combined with hyperaldosteronism and hypokalemia, these phenotypes suggest a more complete closure of chloride shunt conductance. Mechanistically, the positive charge on the amino acid residue K65 in claudin-4 confers anion selectivity (16). Its homologous position in claudin-8 also contains a basic residue (K65), suggesting that claudin-8 may itself function as an anion channel. Because removal of claudin-8 caused concomitant loss of claudin-4 from the TJ, it remained difficult to delineate the claudin-8 role without perturbing the claudin-4 function in vivo. Ubiquitination as a direct mechanism to regulate TJ permeability has been shown before. Takahashi et al. (34) have identified a putative E3 ubiquitin ligase (LNX1p80 from MDCK cells) that interacts with claudin-1 through its PDZ domain and increases the TJ permeability. Mandel et al. (35) have discovered that a fraction of claudin-5 proteins was endogenously ubiquitinated in cultured cerebral endothelial cells. Both studies proposed increased endocytosis as a direct result of claudin ubiquitination. It is important to note that KLHL3 itself can be regulated by angiotensin-II signaling as part of normal physiologic response to volume depletion (36). The physiologic requirement of claudin ubiquitination may suggest that TJ is dynamically remodeled. Shen et al. (37) have made the seminal observation that TJ molecules, such as claudin, occludin, and ZO-1, undergo constant exchange within the TJ or between the TJ and the intracellular milieu. Both extracellular stimuli and intracellular signaling cascades can regulate the turnover rate and the stability of TJ molecules as a means to alter the TJ structure and function (38).

Materials and Methods

The chemicals and antibodies used in this study are summarized in *SI Appendix*, Table S3. All mice were bred and maintained according to the Washington University animal research requirements, and all procedures were approved by the Institutional Animal Research and Care committee. *SI Appendix, Materials and Methods* includes additional topics on generation of claudin-8 floxed animals, animal metabolic studies, hormonal assays and BP measurements, siRNA screening, molecular cloning and retrovirus production, coimmunoprecipitation and ubiquitination assay, and so forth.

ACKNOWLEDGMENTS. We thank Dr. Aubrey Morrison for helpful suggestions on this manuscript. We thank Jiaqi Zhang for maintaining and genotyping transgenic animals. We thank the Hope Center of Washington University for assistance with arterial blood pressure measurements. We also thank the Cardiology Center of Washington University for assistance with telemetric blood pressure measurements. This work was supported by National Institutes of Health Grants R01DK084059 and P30DK079333 and American Heart Association Grant 0930050N.

1. Gordon RD (1986) Syndrome of hypertension and hyperkalemia with normal glomerular filtration rate. *Hypertension* 8(2):93–102.
2. Wilson FH, et al. (2001) Human hypertension caused by mutations in WNK kinases. *Science* 293(5532):1107–1112.
3. Boyden LM, et al. (2012) Mutations in kelch-like 3 and cullin 3 cause hypertension and electrolyte abnormalities. *Nature* 482(7383):98–102.
4. Louis-Dit-Picard H, et al. (2012) KLHL3 mutations cause familial hyperkalemic hypertension by impairing ion transport in the distal nephron. *Nat Genet* 44(4):456–460.
5. McCormick JA, et al. (2011) A SPAK isoform switch modulates renal salt transport and blood pressure. *Cell Metab* 14(3):352–364.
6. Yang CL, Angell J, Mitchell R, Ellison DH (2003) WNK kinases regulate thiazide-sensitive Na-Cl cotransport. *J Clin Invest* 111(7):1039–1045.
7. Shibata S, Zhang J, Puthumana J, Stone KL, Lifton RP (2013) Kelch-like 3 and Cullin 3 regulate electrolyte homeostasis via ubiquitination and degradation of WNK4. *Proc Natl Acad Sci USA* 110(19):7838–7843.
8. Wakabayashi M, et al. (2013) Impaired KLHL3-mediated ubiquitination of WNK4 causes human hypertension. *Cell Reports* 3(3):858–868.
9. Susa K, et al. (2014) Impaired degradation of WNK1 and WNK4 kinases causes PHAII in mutant KLHL3 knock-in mice. *Hum Mol Genet* 23(19):5052–5060.
10. Canessa CM, et al. (1994) Amiloride-sensitive epithelial Na+ channel is made of three homologous subunits. *Nature* 367(6462):463–467.
11. Gong Y, et al. (2014) The Cap1-claudin-4 regulatory pathway is important for renal chloride reabsorption and blood pressure regulation. *Proc Natl Acad Sci USA* 111(36): E3766–E3774.
12. Ring AM, et al. (2007) WNK4 regulates activity of the epithelial Na+ channel in vitro and in vivo. *Proc Natl Acad Sci USA* 104(10):4020–4024.
13. Yamauchi K, et al. (2004) Disease-causing mutant WNK4 increases paracellular chloride permeability and phosphorylates claudins. *Proc Natl Acad Sci USA* 101(13):4690–4694.
14. Kahle KT, et al. (2004) Paracellular Cl- permeability is regulated by WNK4 kinase: Insight into normal physiology and hypertension. *Proc Natl Acad Sci USA* 101(41): 14877–14882.
15. Schambelan M, Sebastian A, Rector FC, Jr (1981) Mineralocorticoid-resistant renal hyperkalemia without salt wasting (type II pseudohypoaldosteronism): Role of increased renal chloride reabsorption. *Kidney Int* 19(5):716–727.
16. Hou J, Renigunta A, Yang J, Waldegger S (2010) Claudin-4 forms paracellular chloride channel in the kidney and requires claudin-8 for tight junction localization. *Proc Natl Acad Sci USA* 107(42):18010–18015.
17. Troy TC, Rahbar R, Arabzadeh A, Cheung RM, Turksen K (2005) Delayed epidermal permeability barrier formation and hair follicle aberrations in Inv-Cldn6 mice. *Mech Dev* 122(6):805–819.
18. Amasheh S, et al. (2009) Na+ absorption defends from paracellular back-leakage by claudin-8 upregulation. *Biochem Biophys Res Commun* 378(1):45–50.
19. Ohtsuki S, Yamaguchi H, Katsukura Y, Asashima T, Terasaki T (2008) mRNA expression levels of tight junction protein genes in mouse brain capillary endothelial cells highly purified by magnetic cell sorting. *J Neurochem* 104(1):147–154.
20. Konrad M, et al. (2006) Mutations in the tight-junction gene claudin 19 (CLDN19) are associated with renal magnesium wasting, renal failure, and severe ocular involvement. *Am J Hum Genet* 79(5):949–957.
21. Loffing J, et al. (2004) Altered renal distal tubule structure and renal Na(+) and Ca(2+) handling in a mouse model for Gitelman's syndrome. *J Am Soc Nephrol* 15(9):2276–2288.
22. Nielsen S, DiGiovanni SR, Christensen EI, Knepper MA, Harris HW (1993) Cellular and subcellular immunolocalization of vasopressin-regulated water channel in rat kidney. *Proc Natl Acad Sci USA* 90(24):11663–11667.
23. Li WY, Huey CL, Yu AS (2004) Expression of claudin-7 and -8 along the mouse nephron. *Am J Physiol Renal Physiol* 286(6):F1063–F1071.
24. Christensen BM, et al. (2010) Sodium and potassium balance depends on αENaC expression in connecting tubule. *J Am Soc Nephrol* 21(11):1942–1951.
25. Ronzaud C, et al. (2007) Impairment of sodium balance in mice deficient in renal principal cell mineralocorticoid receptor. *J Am Soc Nephrol* 18(6):1679–1687.
26. Hou J, et al. (2009) Claudin-16 and claudin-19 interaction is required for their assembly into tight junctions and for renal reabsorption of magnesium. *Proc Natl Acad Sci USA* 106(36):15350–15355.
27. Tatum R, et al. (2010) Renal salt wasting and chronic dehydration in claudin-7-deficient mice. *Am J Physiol Renal Physiol* 298(1):F24–F34.
28. McCormick JA, et al. (2014) Hyperkalemic hypertension-associated cullin 3 promotes WNK signaling by degrading KLHL3. *J Clin Invest* 124(11):4723–4736.
29. Hou J, Gomes AS, Paul DL, Goodenough DA (2006) Study of claudin function by RNA interference. *J Biol Chem* 281(47):36117–36123.
30. Yang SS, et al. (2007) Molecular pathogenesis of pseudohypoaldosteronism type II: Generation and analysis of a Wnk4(D561A/+) knockin mouse model. *Cell Metab* 5(5):331–344.
31. McCormick JA, Nelson JH, Yang CL, Curry JN, Ellison DH (2011) Overexpression of the sodium chloride cotransporter is not sufficient to cause familial hyperkalemic hypertension. *Hypertension* 58(5):888–894.
32. Lalioti MD, et al. (2006) Wnk4 controls blood pressure and potassium homeostasis via regulation of mass and activity of the distal convoluted tubule. *Nat Genet* 38(10): 1124–1132.
33. Hou J, et al. (2008) Claudin-16 and claudin-19 interact and form a cation-selective tight junction complex. *J Clin Invest* 118(2):619–628.
34. Takahashi S, et al. (2009) The E3 ubiquitin ligase LNX1p80 promotes the removal of claudins from tight junctions in MDCK cells. *J Cell Sci* 122(Pt 7):985–994.
35. Mandel I, et al. (2012) The ubiquitin-proteasome pathway regulates claudin 5 degradation. *J Cell Biochem* 113(7):2415–2423.
36. Shibata S, et al. (2014) Angiotensin II signaling via protein kinase C phosphorylates Kelch-like 3, preventing WNK4 degradation. *Proc Natl Acad Sci USA* 111(43): 15556–15561.
37. Shen L, Weber CR, Turner JR (2008) The tight junction protein complex undergoes rapid and continuous molecular remodeling at steady state. *J Cell Biol* 181(4):683–695.
38. Turner JR, Buschmann MM, Romero-Calvo I, Sailer A, Shen L (2014) The role of molecular remodeling in differential regulation of tight junction permeability. *Semin Cell Dev Biol* 36:204–212.